

Landau damping of electrons with bouncing motion in a radio-frequency plasma

Jun Tao(陶军), Nong Xiang(项农), Yemin Hu(胡业民), and Yueheng Huang(黄跃恒)
Citation: Chin. Phys. B, 2021, 30 (**12**): 125202. DOI: 10.1088/1674-1056/ac16cd
Journal homepage: http://cpb.iphy.ac.cn; http://iopscience.iop.org/cpb

What follows is a list of articles you may be interested in

Numerical investigation of radio-frequency negative hydrogen ion sources by a three-dimensional fluid model

Ying-Jie Wang(王英杰), Jia-Wei Huang(黄佳伟), Quan-Zhi Zhang(张权治), Yu-Ru Zhang(张钰如), Fei Gao(高飞), and You-Nian Wang(王友年)
Chin. Phys. B, 2021, 30 (**9**): 095205. DOI: 10.1088/1674-1056/ac0e21

Plasma characteristics and broadband electromagnetic wave absorption in argon and helium capacitively coupled plasma

Wen-Chong Ouyang(欧阳文冲), Qi Liu(刘琦), Tao Jin(金涛), and Zheng-Wei Wu(吴征威)
Chin. Phys. B, 2021, 30 (**9**): 095203. DOI: 10.1088/1674-1056/abeb0d

Synthesis of SiC/graphene nanosheet composites by helicon wave plasma

Jia-Li Chen(陈佳丽), Pei-Yu Ji(季佩宇), Cheng-Gang Jin(金成刚), Lan-Jian Zhuge(诸葛兰剑), and Xue-Mei Wu(吴雪梅)
Chin. Phys. B, 2021, 30 (**7**): 075201. DOI: 10.1088/1674-1056/abe1a1

Numerical simulation and experimental validation of multiphysics field coupling mechanisms for a high power ICP wind tunnel

Ming-Hao Yu(喻明浩), Zhe Wang(王哲), Ze-Yang Qiu(邱泽洋), Bo Lv(吕博), and Bo-Rui Zheng(郑博睿)
Chin. Phys. B, 2021, 30 (**6**): 065201. DOI: 10.1088/1674-1056/abeb0e

Effect of radio frequency bias on plasma characteristics of inductively coupled argon discharge based on fluid simulations

Xiao-Yan Sun(孙晓艳), Yu-Ru Zhang(张钰如), Sen Chai(柴森), You-Nian Wang(王友年), Yan-Yan Chu(楚艳艳), Jian-Xin He(何建新)
Chin. Phys. B, 2020, 29 (**9**): 095203. DOI: 10.1088/1674-1056/ab9436

Landau damping of electrons with bouncing motion in a radio-frequency plasma*

Jun Tao(陶军)[1,2], Nong Xiang(项农)[1,†], Yemin Hu(胡业民)[1,‡], and Yueheng Huang(黄跃恒)[3,4]

[1] *Institute of Plasma Physics, Hefei Institutes of Physical Science, Chinese Academy of Sciences, Hefei* 230031, *China*
[2] *University of Science and Technology of China, Hefei* 230026, *China*
[3] *Advanced Energy Research Center, Shenzhen University, Shenzhen* 518060, *China*
[4] *Key Laboratory of Optoelectronic Devices and Systems of Ministry of Education and Guangdong Province, College of Optoelectronic Engineering, Shenzhen University, Shenzhen* 518060, *China*

(Received 14 May 2021; revised manuscript received 2 July 2021; accepted manuscript online 22 July 2021)

One-dimensional particle simulations have been conducted to study the interaction between a radio-frequency electrostatic wave and electrons with bouncing motion. It is shown that bounce resonance heating can occur at the first few harmonics of the bounce frequency ($n\omega_b, n = 1,2,3,\ldots$). In the parameter regimes in which bounce resonance overlaps with Landau resonance, the higher harmonic bounce resonance may accelerate electrons at the velocity much lower than the wave phase velocity to Landau resonance region, enhancing Landau damping of the wave. Meanwhile, Landau resonance can increase the number of electrons in the lower harmonic bounce resonance region. Thus electrons can be efficiently heated. The result might be applicable for collisionless electron heating in low-temperature plasma discharges.

Keywords: first few harmonics, bounce resonance, Landau resonance, resonance overlaps

PACS: 52.50.Qt, 52.40.−w, 52.65.−y **DOI:** 10.1088/1674-1056/ac16cd

1. Introduction

Inductively coupled discharges and capacitively coupled discharges have been broadly used in the past decades. Inductively coupled discharges are maintained by absorbing the energy of a radio-frequency (RF) electric field excited from an antenna, while capacitively coupled discharges are realized by applying a voltage to the electrodes in contact with the plasma. A large number of theoretical and experimental studies have been carried out on the electron heating mechanism.[1–6] In recent particle-in-cell simulations, the dominant heating mechanism can change under certain conditions even at low pressures, and Ohmic heating may be more dominant.[7,8] However, collisionless electron heating plays an important role in understanding electron power absorption in low-pressure RF plasmas.[9–12]

The problem of collisionless plasma heating appeared about half a century ago and has been extensively studied in theoretical simulations and experiments. In the theory, initially collisionless electron heating as an anomalous skin effect in the half-infinite plasma has been studied by Weibel *et al.* and the non-monotonic decrease in the RF field has been observed.[13–15] Such an important collisionless electron heating mechanism was first popularized by Turner *et al.* and a self-consistent simulation of the electron heating process was performed by assuming that electrons are absorbed as they reach the boundary.[11,16,17] However, for bounded plasmas such as inductively coupled plasma discharges, electrons are reflected back into the plasma region at the plasma boundary by the sheath potential formed between the plasma and wall. For this reason, Shaing developed a kinetic theory to describe the collisionless electron heating in inductively coupled discharges of a finite length.[18] The results show that both the wave-particle resonance and bounce resonance can heat electrons. In the limit that the anomalous skin depth is much small than the plasma length, the wave-particle resonance effect dominates. For the case that the skin depth is comparable to plasma length, the bounce resonance becomes dominant in electron heating. Collisionless electron heating by bounce resonance in a bounded plasmas has been intensively investigated in Refs. [19–24]. In these works, more attention has been paid to the coupling between external RF coils and electric fields induced in the plasma, where collisionless electron heating is quantitatively characterized by the surface impedance. The interaction between electrons and the wave in the presence of both resonances is not clearly described. Besides, they only considered that the waves were incident vertically and the inhomogeneity of the plasma was assumed only in the direction of wave propagation. Subsequently, Angus *et al.* studied the electron heating and transmission of an electromagnetic wave obliquely incident on a bounded plasma,[25] where the electric field in the x-direction and the electric field in the z-

*Project supported by the National Key Research and Development Program of China (Grant No. 2017YFE0300406) and the National Natural Science Foundation of China (Grant Nos. 11975272, 12075276, 11805133, 11705236, and 11375234).

†Corresponding author. E-mail: xiangn@ipp.ac.cn
‡Corresponding author. E-mail: yeminhu@ipp.ac.cn

© 2021 Chinese Physical Society and IOP Publishing Ltd

direction are obtained. Meanwhile, some of the collisionless effects have been observed in RF discharges by self-consistent simulations.[16,26] The simulation results show how the electromagnetic field and current density distribution are altered as a result of the thermal motions of the electrons. In more recent years, fluid, particle and hybrid models have undergone continuous refinements and have been adopted to simulate different aspects of the physics associated with RF discharges. Electron bounce resonance was experimentally investigated by measuring the electron energy probability function (EEPF) distribution in a planar type inductively coupled plasma, and the dependence of EEPF on various finite lengths was presented.[15,27–30] The electron energy distribution function (EEDF) of ballistic electrons was also measured in a DC/RF hybrid capacitively coupled discharge. Landau damping of plasma waves is considered to be the main channel for the growth of the high-energy tail of EEDF.[31]

Bounce resonance of charged particles with waves has also been observed and discussed in other plasmas. For example, in axis-symmetric mirror plasmas, where the electron bounce resonance heating was confirmed and associated radial transport was discussed.[32,33] In tokamaks, global gyrokinetic particle simulation reveals that the enhancement of the geodesic acoustic mode damping (GAM) rate is due to resonance between the GAM oscillation and the trapped electron bounce motion.[34,35] The electron bounce motion caused by secondary electrons is presented in Ref. [36], where the presence of high-energy ballistic electrons (HEBEs) originating form secondary electrons in a low-pressure RF plasma, as well as the ballistic nature of HEBEs and their typical bouncing characteristics between RF sheaths, were demonstrated by full-kinetic PIC simulations.

Up to date, although different plasma-wave resonances in bounded plasmas have been demonstrated, few cases have been discussed when different plasma-wave resonances simultaneously exist. The simultaneous existence of different plasma-wave resonances have been observed in tokamak plasma. For example, the interactions between the electron cyclotron resonance and Landau damping of a lower hybrid wave, between two lower hybrid waves.[37–39] In spite of the fact that the heating mechanisms of Landau resonance and bounce resonance have been shown, the effect on energy transfer between the electric field and charged particles when both resonances are present is not clearly illustrated, especially how the Landau damping is affected by the bounce resonance and vice verse. In this paper, the interaction of an electrostatic wave and electrons in a bounded plasma is investigated by particle simulations when Landau and bounce resonance are present simultaneously. The synergy effects of the bounce resonance and Landau resonance on collisionless electron heating are discussed in detail. It is found that the Landau damping and bounce resonance can be enhanced, and so electrons can be heated efficiently.

The remainder of the paper is organized as follows. The dispersion relation for waves propagating in parallel directions is described in Section 2. In Section 3, the interaction between the wave and electrons when the two resonance regions overlap is investigated by particle simulation. Finally, the main results are summarized in Section 4.

2. Physical model

Our physical model assumes one-dimensional space, three-dimensional velocity, slab geometry, and the isotropic homogeneous plasma are confined in the region $0 \le z \le L$. The kinetic equation for electron distribution function f is

$$\frac{\partial f}{\partial t} + \boldsymbol{V}\cdot\nabla f - \frac{e}{m}\boldsymbol{E}\cdot\frac{\partial f}{\partial \boldsymbol{V}} = C(f), \tag{1}$$

where the collision operator is approximated using the Krook model $C(f) = -\nu f$, where ν is the electron collision frequency. The classical analytical approach is to deal with perturbations of a uniform plasma by linearizing, and assuming that the perturbed distribution $f_1(z,t) = f_1(z)\exp(\mathrm{i}\omega t)$ and the electric field $\boldsymbol{E}_1(z,t) = \boldsymbol{E}_1(z)\exp(\mathrm{i}\omega t)$. In the Shaing *et al.*'s model,[18] the response of the vertical electric field is investigated. Here we consider the response of the electric field in the parallel propagation direction at low densities. The linearized Vlasov equation for the perturbed electron distribution in response to the z-direction wave electric field is

$$\mathrm{i}\omega f_1 + V_z\frac{\partial f_1}{\partial z} - \frac{e}{m}E_z\frac{\partial f_0}{\partial V_z} = -\nu f_1, \tag{2}$$

where $f_0 = \frac{N}{(\sqrt{\pi}v_\mathrm{t})^3}\exp\left(-\frac{V^2}{v_\mathrm{t}^2}\right)$ is the Maxwellian velocity distribution function, N is the plasma density, v_t is the electron thermal velocity. We assume that the system length L is much larger than the width of plasma sheath at $z = 0$ and $z = L$, so that the electrons are assumed to be specularly reflected, the boundary conditions are expressed as $f_1(V_z > 0, z = 0) = f_1(V_z < 0, z = 0)$ and $f_1(V_z > 0, z = L) = f_1(V_z < 0, z = L)$. By the boundary condition, the perturbed distribution function becomes

$$f_1(z) = \left[\int_L^z \frac{D(V_z,z')}{V_z}\exp(a_\nu z')\,\mathrm{d}z' + G(V_z)\right]\exp(-a_\nu z), \tag{3}$$

where

$$D(V_z,z') = \frac{eE_z}{m}\frac{\partial f_0}{\partial V_z},\quad a_\nu = \frac{\mathrm{i}\omega+\nu}{V_z},$$

$$G(V_z) = \frac{\int_L^0 \frac{D(V_z,z')}{Vz}\left[\exp(-a_\nu z') - \exp(a_\nu z')\right]\mathrm{d}z'}{1-\exp(-2a_\nu L)}.$$

Extending the domain from $0 \le z \le L$ to $-L \le z \le L$, and the wave electric field $E_z(-z) = -E_z(z)$. In order to perform

the velocity space integral, we adopt the spherical coordinates (V,θ,ϕ) for the velocity space such that $V_z = V\cos\theta$, and the current density J_z in the expanded domain can be calculated by

$$J_z = \frac{4Ne^2}{m\sqrt{\pi}v_t}\int_{-L}^{L} E_z(z')\,K(|z-z'|)\,\mathrm{d}z', \tag{4}$$

where

$$K(|z-z'|) = \int_0^{\infty} x^3\exp(-x^2)\,\mathrm{d}x \times \int_0^{\frac{\pi}{2}} \Phi(|z-z'|)\,\frac{\sin\theta\cos\theta}{1-\exp\left(-\frac{2a_\nu L}{x\cos\theta}\right)}\,\mathrm{d}\theta. \tag{5}$$

In Eq. (5), $x = \frac{V}{v_t}$ and $\Phi(|z-z'|) = \exp\left(-\frac{a_\nu}{x\cos\theta}|z-z'|\right) + \exp\left(-\frac{2a_\nu L}{x\cos\theta}\right)\exp\left(\frac{a_\nu}{x\cos\theta}|z-z'|\right)$. Since a RF electric field can be decomposed into a series of plane waves, we assume in expanded domain in the form of an odd Fourier series for $E_z(z) = \sum_{m=0}^{\infty} a_m \sin(k_m z)$. For a single plane wave with wave number k_m, the corresponding dispersion relation can be obtained in the collisionless limit $\nu/\omega \ll 1$

$$1 - \frac{2\omega_{pe}^2}{\sqrt{\pi}\omega^2 v_t}\int_0^{\infty}\frac{V_z^2}{v_t^2}\exp\left(-\frac{V_z^2}{v_t^2}\right) \times\left[\frac{2\omega}{\omega^2-k_m^2V_z^2} - \frac{2k_mV_z\sin(k_mL)}{(\omega^2-k_m^2V_z^2)\sin\left(\frac{\omega L}{V_z}\right)}\right]\mathrm{d}V_z = 0, \tag{6}$$

where two types of resonance can occur by Eq. (6). The first term in the square brackets of the equation contains Landau damping. The electrons near the wave phase velocity interact with the wave and gain energy from it. The second term shows the bounce resonance that occurs when an electron traverses across the length L in a time equal to a multiple of the wave half period, where $T = 2\pi/\omega$ is the wave period. Bounce resonance is directly related to the length L, and the electron heating is mainly determined by bounce resonance electrons with velocities $V_n = \frac{\omega L}{n\pi}$, with $n = 1,2,3,\ldots$.

In Eq. (6), the two resonances occur simultaneously in a certain parameter region. In the following simulations, an electrostatic wave with the form $E_z = E_0\sin(kz-\omega t)$ is assumed in the low-density plasma and the wave amplitude is constant in time. In the collisionless limit $\nu/\omega \ll 1$, the effect of the two resonances is shown through the electron velocity distribution function. The interaction between electrons and the wave will be discussed in detail when the two resonances overlap.

3. Simulation setup and simulation results

The particle simulation is carried out in one-dimensional geometric space and velocity space, and initially Maxwellian distribution of electrons and ions are uniformly loaded along the z-direction. Only electron motions are traced, and ions are regarded as an unvarying background.

The equations of motion in the wave field are given by

$$m\frac{\mathrm{d}V_z}{\mathrm{d}t} = -eE_0\sin(kz-\omega t), \tag{7}$$

$$\frac{\mathrm{d}z}{\mathrm{d}t} = V_z. \tag{8}$$

To preserve the area in the phase space, the symplectic Euler method is used to solve the motion equations (7) and (8),

$$V_{n+1} = V_n - \frac{eE_0\sin(kz_n-\omega t_n)}{m}\Delta t, \tag{9}$$

$$z_{n+1} = z_n + V_{n+1}\Delta t. \tag{10}$$

The simulation parameters are chosen as used in a plasma discharge listed as follows. The spatial length of simulation domain is $L = 21$ cm and the electron temperatures $T_e = 3$ eV, and $\omega = 2\pi\times 13.56$ MHz.

To demonstrate how Landau damping is affected by bounce resonance, four cases are simulated and discussed. An electric field amplitude $E_0 = 40$ V/m is used in the cases 1–3 to investigate the effects of resonance overlaps on plasma-wave interactions. Landau damping is shown in case 1, where the wave number $k = 36.5$ m^{-1} and the wave phase velocity $\omega/(kV_t) = 3.2$, where $V_t = \sqrt{T_e/m}$ is the electron thermal speed. The boundary conditions are periodic, and the interaction of electrons with wave is only through the Landau damping. In case 2, electrons are reflected at two boundaries. The reduction of wave number k and the wave phase velocity $\omega/(kV_t) = 6.4 \gg 1$, which results in few electrons can satisfy the resonant condition $\omega = kV_z$. As shown in Eq. (6), for an electron at a velocity V_z, the bounce resonance condition $\omega = n\pi L/V_z$ and the corresponding bounce resonance velocity $V_n/V_t = 7.8/n$, with $n = 1,2,3,\ldots$. It indicates that electrons can resonant with the wave only by bouncing motion. In case 3, the phase velocity $V_p = 3.2V_t$ and the boundary conditions are the same as in case 2, where electrons interact with the wave by the Landau damping and bounce resonance. Since the resonance half-width of two resonances is proportional to the electric field amplitude, a small resonance overlap is obtained in case 4 by reducing the electric field amplitude based on case 3. These simulation results will be presented and explained in the next section.

3.1. Motions of electrons in the presence of Landau damping

In order to show how the Landau resonance is affected by bounce resonances, we first show the plasma-wave interaction when only Landau resonance is present. Landau damping is caused by resonant interactions of particles with velocities

comparable to the wave phase velocity. In this process, these resonant particles exchange energy with the wave. Electrons slower than the phase velocity are accelerated, so the energy of the wave is absorbed by the electrons. Conversely, electrons fasters than the phase velocity are slowed down, so the energy of the electrons is absorbed by the wave. Figure 1 shows the contour plots of the electron distribution in the phase space and the corresponding parallel velocity distribution function (spatially averaged) at times $t/T = 1.25, 2.25, 3.5, 15$, in which electrons resonate with the wave only through Landau damping. The electron distribution in phase space gradually forms a vortex structure around the phase velocity $V_\mathrm{p} = 3.2V_\mathrm{t}$, and the resonance half-width is $\Delta V = 2\sqrt{\frac{eE_0}{mk}}$. The resonant width is shown by black dashed lines in the phase space. As time increases, the electron velocity distribution function deviates significantly from the initial Maxwellian distribution at $V_z/V_\mathrm{t} > 0$, and a plateau can be formed along the direction of the wave propagation.

3.2. Motions of electrons in the presence of bounce resonance

In Section 2, it is shown that the resonance between electrons with bouncing motion and the wave in a collisionless finite length system leads to electron heating. For a slab of width L, the bounce period for an electron with velocity V_z is $T_\mathrm{b} = 2L/V_z$, and the harmonic bounce resonance occurs when the wave frequency is equal to a multiple of the bounce frequency ($\omega = n\omega_\mathrm{b}, n = 1, 2, 3, \ldots$). In Fig. 2, cases 2 shows the bounce resonance electrons with velocities $V_n = 7.8V_\mathrm{t}/n$ and few electrons can satisfy such a high phase velocity $V_\mathrm{p} = 6.4V_\mathrm{t}$. It indicates that electrons interact with the wave predominantly through bounce resonance. The evolution of electrons in phase space and the corresponding parallel velocity distribution functions at times $t/T = 1.25, 2.25, 3.5, 15$ are shown. The electron distribution in the phase space around the harmonic bounce resonance velocity for $n = 2$ gradually forms

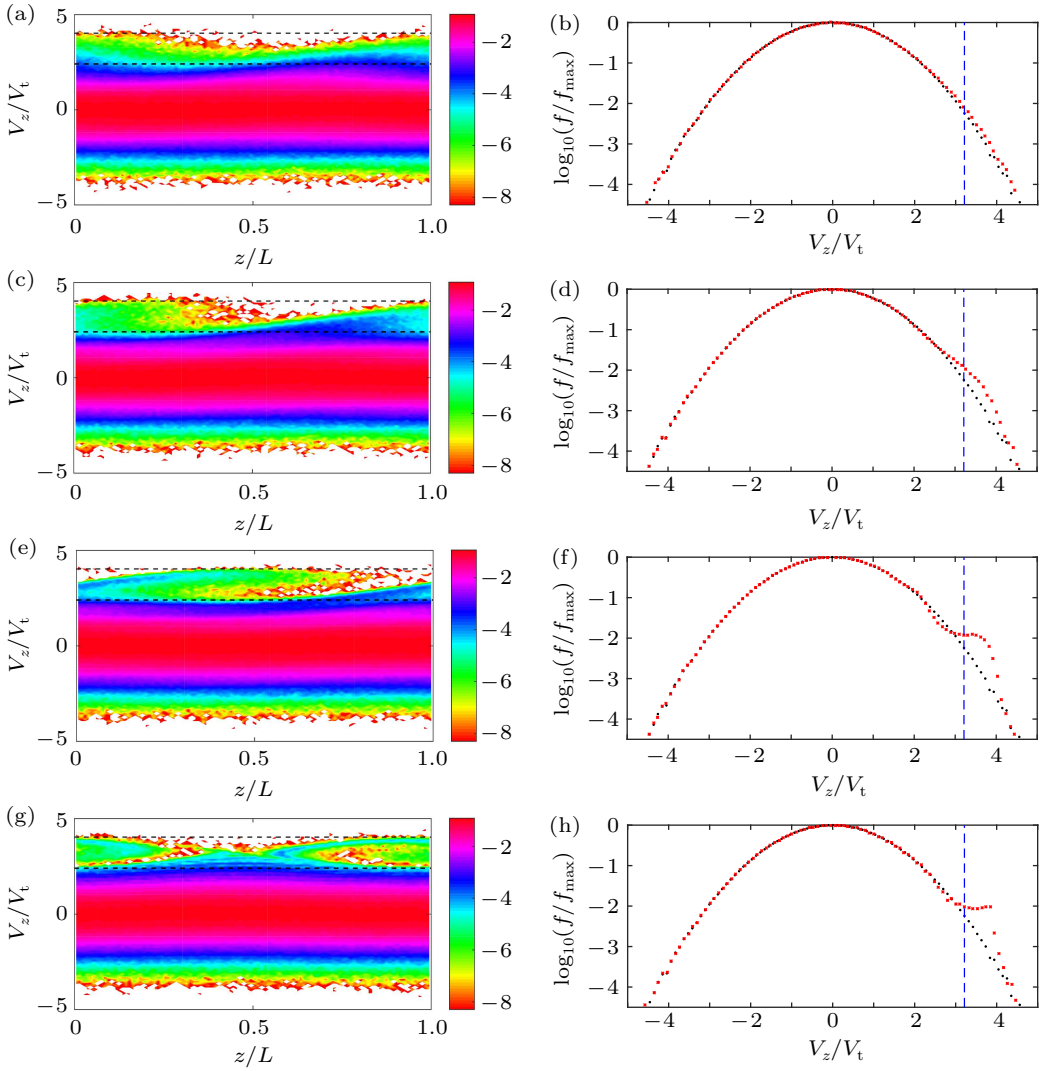


Fig. 1. The contour plots of the electron distribution in the phase space (z, V_z) and the corresponding spatially averaged parallel velocity distribution functions (the red asterisks) at times $t/T = 1.25, 2.25, 3.5, 15$. All distribution functions are plotted on a logarithmic scale and the electron velocity is normalized to the electron thermal velocity. The black circles show the Maxwellian distribution functions, and the blue dashed lines show the resonant phase velocity $V_\mathrm{p} = 3.2V_\mathrm{t}$.

a vortex structure similar to that in Fig. 1. Electrons with velocities lower than V_n are accelerated to larger velocities and the corresponding velocity distribution functions deviate significantly from the initial Maxwellian distribution. Plateaus are formed on both sides of the velocity distribution function due to the bounce motion. There are almost no electrons around the harmonic bounce resonance velocity for $n = 1$, which is not shown here. In Fig. 2(h), although there are more particles around the harmonic bounce resonance velocity for $n = 3$, only a small plateau is formed, and it is difficult for higher harmonic bounce resonances to appear. The particle velocity distribution was experimentally measured by coherent laser induced fluorescence (LIF) techniques, and a plateau was also observed around the third harmonic bounce resonance velocity.[40] The simulation results show that bounce resonance occurs preferentially at the first few harmonic frequencies, while the response of higher harmonic bounce resonances tends to be weaker.

To understand the dependence of the intensity of bounce effect on the resonance velocity, the evolution of the electric field and V_z^2/V_t^2 for two electrons with different initial conditions are shown in Fig. 3. In Fig. 3(a), an electron with initial velocity $V_0 = 3.6V_t$ can be observed traversing length L for a time equal to two times the wave half period, which indicates that the electron can interact with the wave through second harmonic bounce resonance. Meanwhile, the electron with initial velocity $V_0 = 2.5V_t$ is accelerated through third harmonic bounce resonance, as shown in Fig. 3(b). The electron in the second harmonic bounce resonance region have a longer in-phase acceleration time and can be effectively accelerated. For the electron with initial velocity $V_0 = 2.5V_t$, the in-phase acceleration time becomes shorter when traversing the length L, so the wave and electron interaction is very weak. Because of this, the plateau near the third harmonic bounce resonance velocity is not very obvious in Fig. 2(h). For the bounce resonance with $n \geq 4$, although there are more resonant particles, the in-phase acceleration time becomes less, resulting in these resonant particles not gaining energy effectively. As a result, electron heating is mainly contributed by bounce resonance of the first few harmonics. This results agrees with that obtained in the Ref. [41].

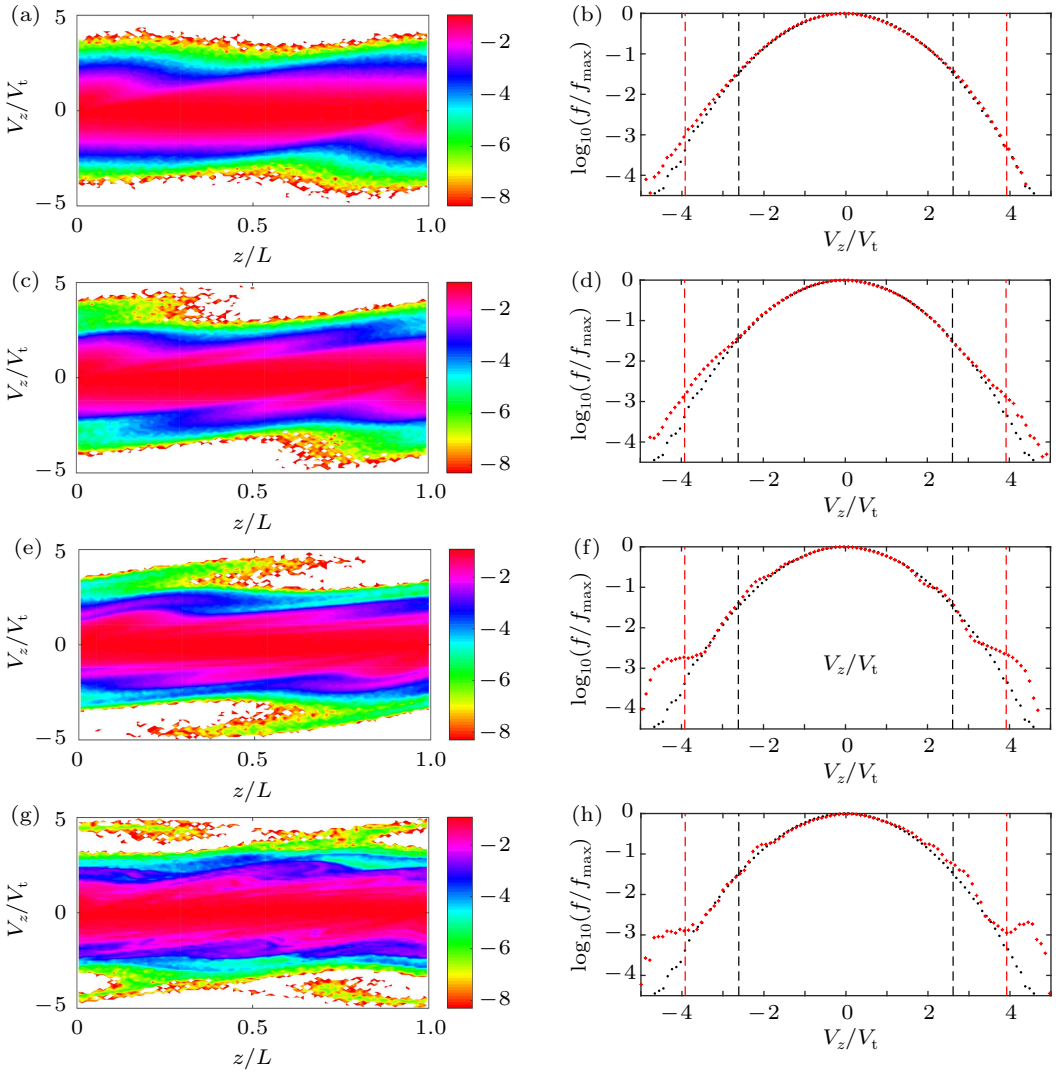


Fig. 2. Resulting electron distributions at times $t/T = 1.25, 2.25, 3.5, 15$ obtained from case 2. The red and black dashed lines on the velocity distribution show the second harmonic bounce resonance velocity and third harmonic bounce resonance velocity based on the theoretical prediction, respectively.

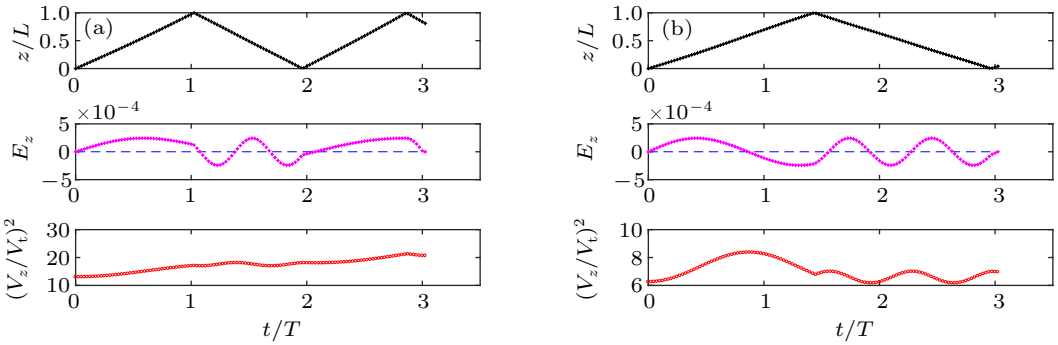


Fig. 3. The evolution of the electric field and V_z^2/V_t^2 for two electrons with different initial conditions.

3.3. Interaction of electrons and wave in the presence of bounce resonance and Landau damping

The particle simulation results for case 3 are shown in Fig. 4, in which electrons interact with the wave through Landau damping and bounce resonance. Figure 4 shows the resulting electron phase space distribution and the corresponding parallel velocity distributions at times $t/T = 1.25, 2.25, 3.5, 15$. Since both the second harmonic bounce resonance velocity (V_2) and the third harmonic bounce resonance velocity (V_3) are in the Landau resonance region $(V_p - \Delta V, V_p + \Delta V)$, the Landau resonance half-width is $\Delta V = 2\sqrt{\frac{eE_0}{mk}}$, which indicates that the two types of resonance overlap. Electrons accelerated through bounce resonance may be affected by Landau damping. In Fig. 4(b), electrons interact with wave only through Landau damping at $t \leq T$, resulting in the velocity distribution function deviates from the Maxwellian distribution on the $V_z/V_t > 0$ side, which is different from those in Fig. 2(b).

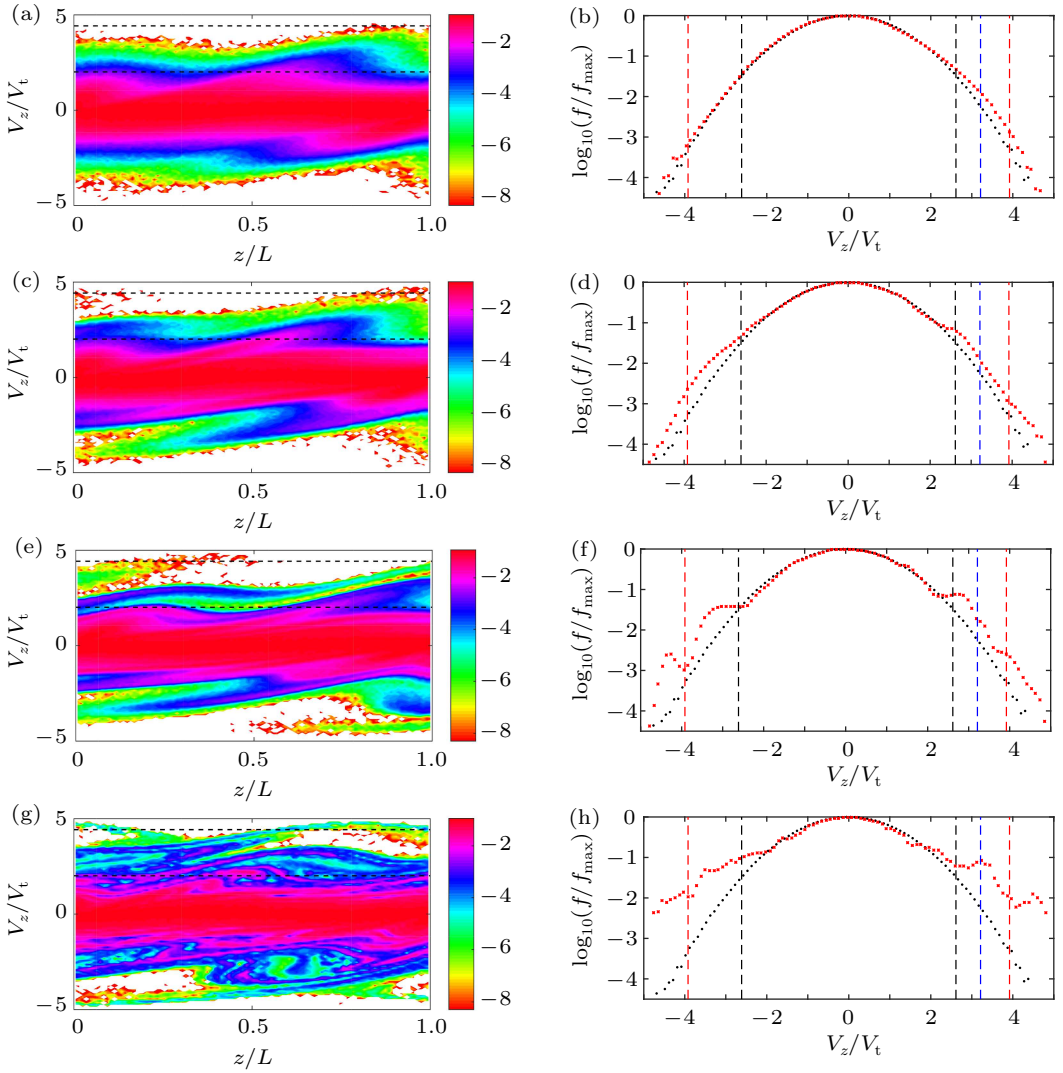


Fig. 4. Resulting electron distributions at times $t/T = 1.25, 2.25, 3.5, 15$ obtained from case 3. Landau resonant width is shown by the black dashed lines in the phase space. The resonant phase velocity, second harmonic bounce resonance velocity and third harmonic bounce resonance velocity are shown by blue, red and black dashed lines, respectively.

In Fig. 4(d), a plateau appears on both sides of the velocity distribution around the second harmonic bounce resonance velocity. On the $V_z/V_t > 0$ side, the electron velocity distribution function near phase velocity is significantly different from that in Fig. 1(d). It can be seen that the resonance plateau becomes lower, which means few electrons and weaker interactions around the phase velocity. The reason for this difference is that electrons near the phase velocity do not interact with wave through Landau damping when they are reflected at $z = L$. Therefore, the number of resonant particles is reduced and the Landau damping is weakened. Meanwhile, a small plateau appears on both sides of the velocity distribution function near the second harmonic bounce resonance velocity, which is similar to that in Fig. 2(d).

In Fig. 4(e), electron distribution in the phase space gradually forms multiple vortex structures. Electrons interact with the wave through Landau damping, second harmonic bounce resonance and third harmonic bounce resonance are shown in Fig. 4(f). A significant plateau around the third harmonic bounce resonance velocity is formed, different from that in Fig. 2(f). This phenomenon indicates that the resonant electrons around the third harmonic bounce resonance velocity are affected and the original bounce resonance orbits are gradually destroyed. Since Landau damping occurs only on the right side, the reflected electrons at the boundary deviate from their orbits and the phase space structure gradually changes, leading to the asymmetry of velocity distribution functions on both sides. As time increases, it can be seen that in Fig. 4(g), the low velocity electrons can be efficiently accelerated to higher velocities, and the corresponding plateau of velocity distribution becomes almost flat, as shown in Fig. 4(h).

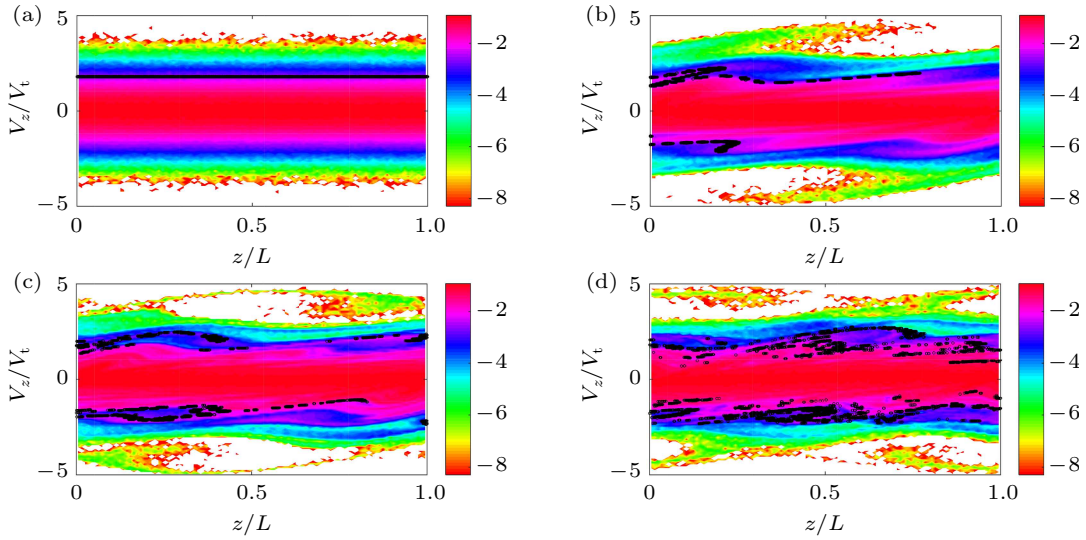


Fig. 5. The evolution of the electron phase space distribution at times $t/T = 0, 3.5, 7.5, 15$ obtained from case 2. The black circles show the trajectory of electrons with initial velocity $V_0 = 1.8V_t$ in phase space.

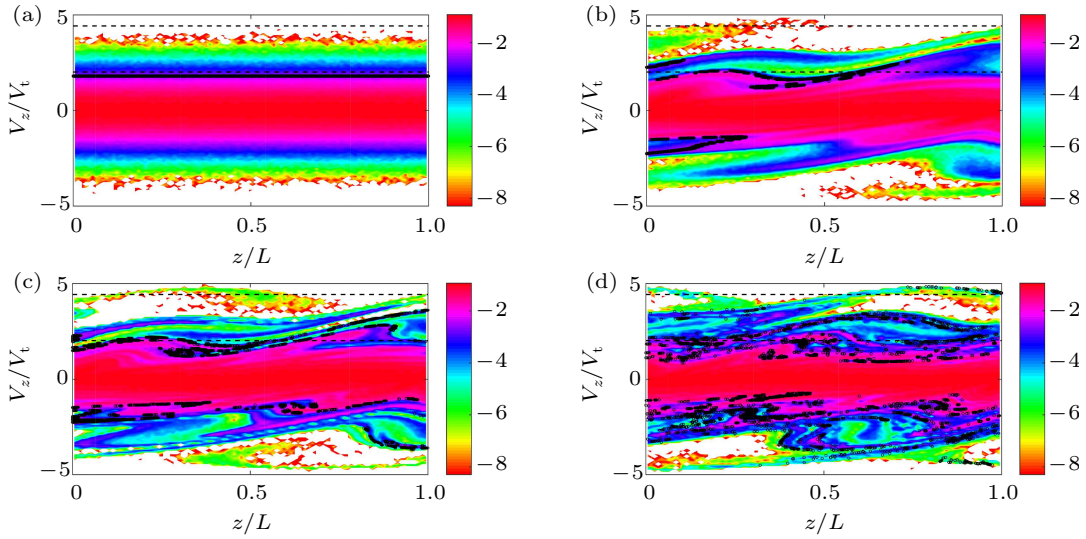


Fig. 6. The evolution of the electron phase space distribution at times $t/T = 0, 3.5, 7.5, 15$ obtained from case 3. The black circles show the trajectory of electrons with initial velocity $V_0 = 1.8V_t$ in phase space.

To demonstrate how electrons in the different resonance regions are affected by resonance overlapping, we plot the trajectories of electrons with different initial velocities. First, we consider the electrons with a initial velocity $V_0 = 1.8V_t$ that are in the third harmonic bounce resonance region and outside the Landau resonance region. As Landau damping is absent in case 2, and the trajectory of electrons with initial velocity $V_0 = 1.8V_t$ (the black circles) in phase space are shown in Fig. 5. In Fig. 5(d), it can be seen that electrons with initial velocity $V_0 = 1.8V_t$ are almost trapped in third harmonic bounce resonance velocity frame. Considering the overlap between the third harmonic bounce resonance and the Landau resonance in case 3, the corresponding trajectories of the electrons with the same initial velocity are shown in Fig. 6. It is significantly different from those in Fig. 5. In Fig. 6(b), the electrons are initially accelerated by bounce resonance. As time increases, the accelerated electrons move into the Landau resonance region and gradually deviate from their original resonant orbits. More electrons are affected by Landau damping, resulting in a longer in-phase acceleration time and a net increase in the kinetic energy for these resonant electrons. Therefore, when the third harmonic bounce resonance region overlaps with the Landau resonance region, low-velocity particles can be accelerated to the Landau resonance region by the bounce resonance and then accelerated by Landau damping. Such a process enhances the Landau damping of wave and resonant particles are accelerated more effectively.

Secondly, the trajectories of electrons with initial velocity $V_0 = 2.7V_t$ (the black circles) in phase space can be obtained from case 2 and case 3. In Fig. 7(d), the electrons with initial velocity $V_0 = 2.7V_t$ are almost trapped in the third harmonic bounce resonance velocity frame, which indicates that these electrons are not in the second harmonic bounce resonance region. In Fig. 8, these electrons with initial velocity $V_0 = 2.7V_t$ are in the Landau resonance region and are accelerated through

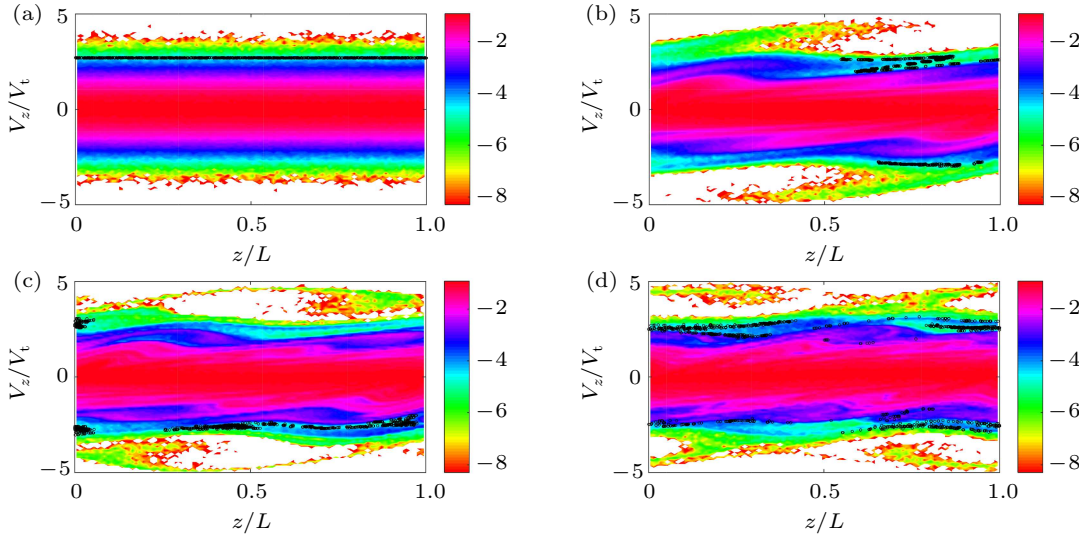


Fig. 7. The evolution of the electron phase space distribution at times $t/T = 0, 3.5, 7.5, 15$ obtained from case 2. The black circles show the trajectory of electrons with initial velocity $V_0 = 2.7V_t$ in phase space.

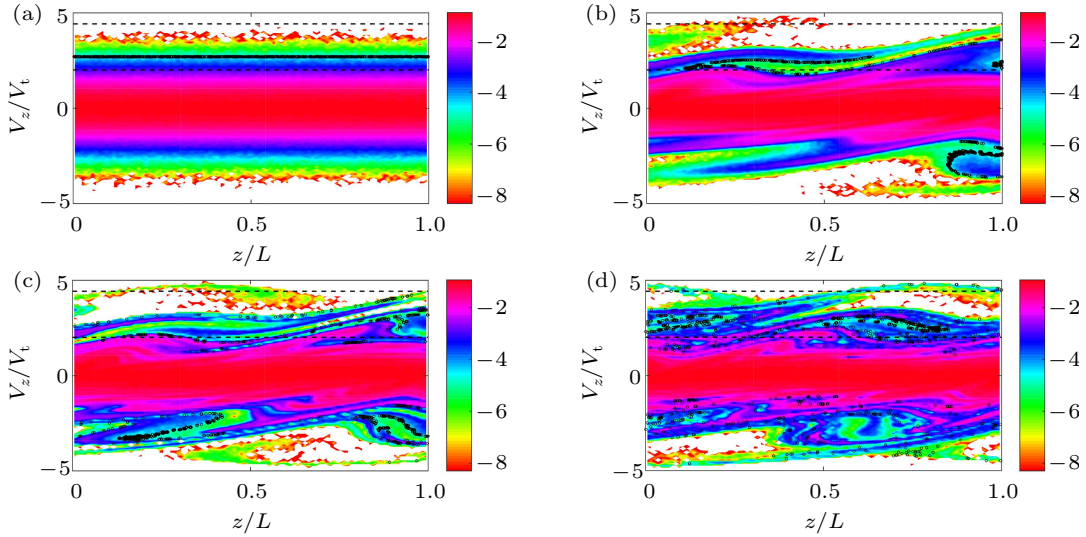


Fig. 8. The evolution of the electron phase space distribution at times $t/T = 0, 3.5, 7.5, 15$ obtained from case 3. The black circles show the trajectory of electrons with initial velocity $V_0 = 2.7V_t$ in phase space.

Landau damping. Since the second harmonic bounce resonance region also overlaps with Landau resonance region, the electrons can also interact with the wave through second harmonic bounce resonance. As shown in Fig. 8(d), the electrons are accelerated beyond the Landau resonance region. Therefore, when the second harmonic bounce resonance region overlaps with the Landau resonance region, the Landau resonance can increase the lower harmonics of electrons in the bounce resonance, resulting in a flattened velocity distribution function and significantly enhanced electron heating.

The temporal evolution of the total kinetic energy of the particles for the three cases is plotted in Fig. 9. For case 1, the linear growth of total kinetic energy of the particles and the subsequent nonlinear oscillations are consistent with the predictions of O'Neil's theory.[42] For $t \leq T$, the variation of kinetic energy is the same for case 1 and case 3, which indicates that the interaction between electrons and wave is mainly through Landau damping. As time increases, the electron heating becomes more pronounced in the presence of the bounce resonance and the Landau damping, as shown in cases 2 and 3 of Fig. 9.

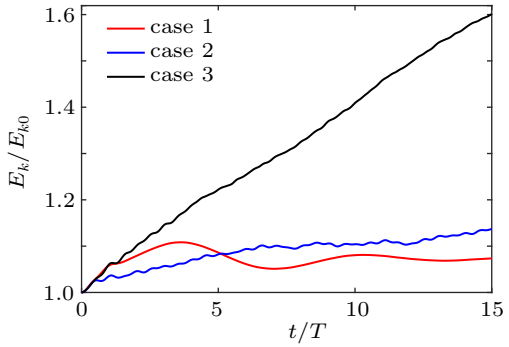


Fig. 9. The temporal evolution of the total kinetic energy of the particles for the three cases. The red solid line in case 1, case 2 and case 3 are blue solid lines and black solid lines, respectively.

3.4. Electron-wave interactions in the presence of weak resonance overlap for bounce resonance and Landau damping

In this case, the amplitude of the resonant wave is reduced to half of the previous amplitude compared to case 3, which leads to a weak resonance overlap. Figure 10 shows the resulting electron distributions from the small electric field amplitude in the same format as plots (a)–(h) in Fig. 4.

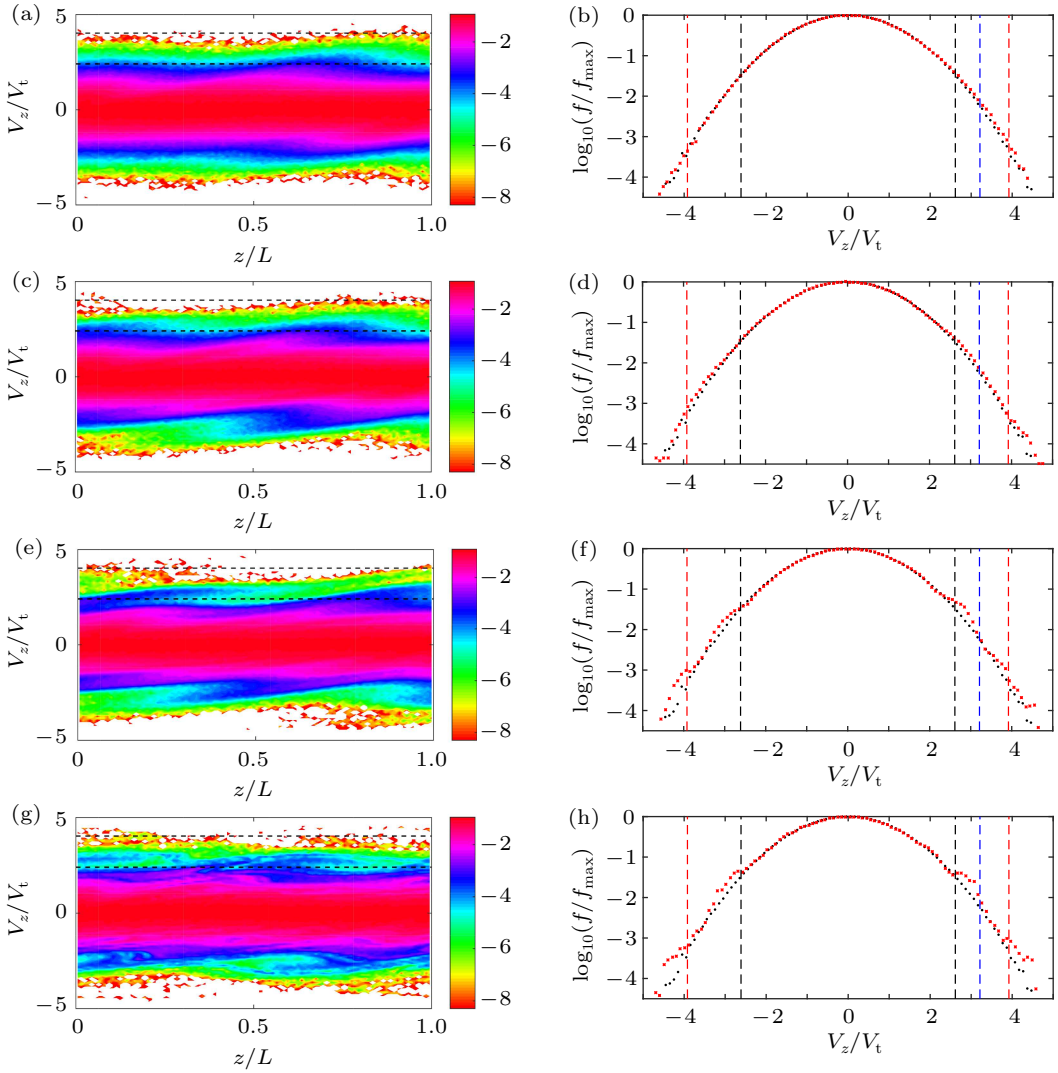


Fig. 10. Resulting electron distributions obtained from the small electric field amplitude. Plots (a)–(h) are in the same format as those in Fig. 4.

In Fig. 10(h), the velocity distribution function is not flattened, which is different from those in Fig. 4(h). This difference is due to the weak resonance overlap between the bounce resonance region and Landau resonance region, resulting in a reduction in the number of electrons accelerated through the third harmonic bounce resonance into the Landau resonance region. The number of electrons accelerated through the Landau damping decreases, and the number of electrons in the bounce resonance for $n = 2$ decreases accordingly. As a result, for such a small electric field amplitude, the resonant width becomes smaller and the overlap of the two resonances is also reduced accordingly, resulting in the resonant electrons cannot be effectively accelerated and electron heating process is not pronounced.

The corresponding kinetic energy evolution is shown in Fig. 11. It can be seen that the electron heating is weak at small electric field amplitudes. Compared to Fig. 9, the oscillatory behavior of the kinetic energy appears when the bounce resonance and Landau damping occur simultaneously. The reason is that when the wave amplitude is small enough, the overlap of bounce resonance and Landau damping becomes smaller and the low-velocity electrons cannot continue to be accelerated through the bounce resonance and Landau damping as before. For the decaying part of the kinetic energy, which is due to nonlinear Landau damping.

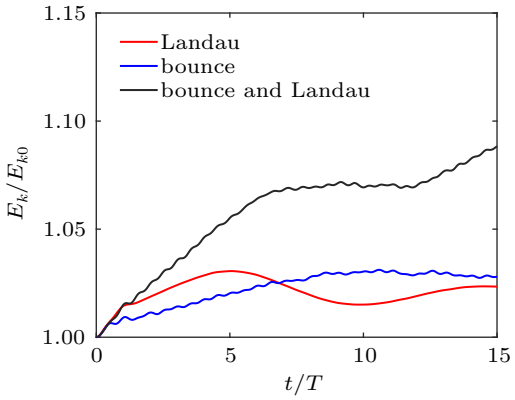


Fig. 11. The evolution of particle kinetic energy with time for the three cases.

4. Summary

In this paper, the interaction between wave and electrons with bouncing motion is investigated theoretically as well as in one-dimensional particle simulation. The synergy effects of the bounce resonance and Landau resonance on collisionless electron heating are investigated, and the energy transfer between electrons and wave as the two resonances overlap is discussed. The results show that both Landau damping and bounce resonance can be enhanced and so the electrons can be heated efficiently.

First, the linearized kinetic equation for the perturbed electron distribution is solved by considering the reflection of electrons at the plasma boundary. The corresponding dispersion relations is obtained by combining Faraday's law and Ampere's law. The analysis results show that both Landau damping and bounce resonance can occur. Four cases are studied by particle simulations to show the electron-wave interactions when two resonances are present simultaneously.

Our simulation results show that the distribution of electrons in the phase space can gradually form a vortex structure near each bounce resonance velocity, and the velocity distribution function forms a plateau near the corresponding bounce resonance velocity. Electrons near each bounce resonance velocity interact the wave and absorb the wave energy. Since the in-phase acceleration time of electrons with higher harmonic bounce resonance is short, so the bounce resonance occurs preferentially at the first few harmonics. For the bounce resonance with $n \geq 4$, resonant electrons are difficult to obtain an effective acceleration. Thus, as the width L increases, the corresponding first few harmonics of bounce resonance velocity increases and the number of resonant electrons decreases, leading to a weaker bounce effect. When size $L \to \infty$ or $\omega \gg \omega_b$, the bounce resonance effect can be ignored.

For such an overlap between the Landau resonance and the bounce resonance, the motion of electrons in the resonant region may be affected by both resonances. As the electrons are reflected at $z = L$, the electrons initially in the Landau resonance region no longer interact with the wave through the Landau damping, and the Landau damping is weakened. As time increases, electrons near the third harmonic bounce resonance velocity will be accelerated by the bounce resonance. Since the two resonances overlap, the electron orbits of higher harmonic bounce resonance are significantly perturbed by the Landau damping, and the resonant electrons can be effectively accelerated. Meanwhile the Landau resonance can increase the number of electrons in the lower harmonic bounce resonant region, resulting in a net increase in the kinetic energy of electrons in each resonant region. Such a process leads to a longer in-phase acceleration time for this part of the resonant electrons and significant change in the distribution function. Eventually, the electron distribution functions on both sides can be elevated. Since the resonant width is proportional to the electric field amplitude, when the electric field amplitude is reduced, the resonant width becomes smaller and the overlap of the two resonances is reduced. As a result, the number of particles interacting with the two resonances decreases, leading to a weakening of the interaction.

Although the heating mechanisms of bounce resonance and Landau resonance have been observed experimentally by measuring the EEPF, the energy transfer between the electric field and electrons has not been clear illustrated. The present study demonstrates that the energy transfer between the electric field and electrons is more effectively when both resonances are present simultaneously. Since the two resonance

regions overlap, the higher harmonic bounce resonance can accelerate the electrons whose velocity is much lower than the wave phase velocity to the Landau resonance region, enhancing the Landau damping of the wave. At the same time, more resonant electrons are accelerated to the lower harmonic bounce resonance region by the Landau resonance.

References

[1] Piejak R B, Godyak V A and Alexandrovich B M 1992 *Plasma Sources Sci. Technol.* **1** 179
[2] Raizer Y P, Shneider M N and Yatsenko N A 1995 *Radio Frequency Capacitive Discharges* (Boca Raton: CRC Press)
[3] Vahedi V, Lieberman M A, Dipeso G, Rognlien T D and Hewett D 1995 *J. Appl. Phys.* **78** 1446
[4] Godyak V A, Piejak R B, Alexandrovich B M and Kolobov V I 1998 *Phys. Rev. Lett.* **80** 3264
[5] You S J, Chung C W and Chang H Y 2005 *Appl. Phys. Lett.* **87** 041501
[6] Sun A, Becker M M and Loffhagen D 2016 *Comput. Phys. Comm.* **206** 35
[7] Fu Y Y, Zheng B C, Wen D Q, Zhang P, Fan Q H and Verboncoeur J P 2020 *Appl. Phys. Lett.* **117** 204101
[8] Vass M, Wilczek S, Lafleur T, Brinkmann R P, Donko Z and Schulze J 2020 *Plasma Sources Sci. Technol.* **29** 085014
[9] Hopwood J, Guarnieri C R, Whitehair S J and Cuomo J J 1993 *J. Vac. Sci. Technol. A* **11** 147
[10] Hopwood J, Guarnieri C R, Whitehair S J and Cuomo J J 1993 *J. Vac. Sci. Technol. A* **11** 152
[11] Turner M M 1993 *Phys. Rev. Lett.* **71** 1844
[12] Barnes M S, Forster J C and Keller J H 1993 *Appl. Phys. lett.* **62** 2622
[13] Weibel E S 1967 *Phys. Fluids* **10** 741
[14] Blevin H A, Reynolds J A and Thonemann P C 1970 *Phys. Fluids* **13** 1259
[15] Godyak V A and Kolobov V I 1998 *Phys. Rev. Lett.* **81** 369
[16] Turner M M 1996 *Plasma Sources Sci. Technol.* **5** 159
[17] Turner M M 2009 *J. Phys. D: Appl. Phys.* **42** 194008
[18] Shaing K C and Aydemir A Y 1997 *Phys. Plasmas* **4** 3163
[19] Yoon N S, Kim S S, Chang C S and Choi D I 1996 *Phys. Rev. E* **54** 757
[20] Kaganovich I D, Kolobov V I and Tsendin L D 1996 *Appl. Phys. Lett.* **69** 3818
[21] Aliev Y M, Kaganovich I D and Schlüter H 1997 *Phys. Plasmas* **4** 2413
[22] Chung C W, Kim S S, Seo S H, Chang H Y and Yoon N S 2000 *J. Appl. Phys.* **88** 1181
[23] Chung C W, You K I, Seo S H, Kim S S and Chang H Y 2001 *Phys. Plasmas* **8** 2992
[24] Kaganovich I D, Polomarov O V and Theodosiou C E 2004 *Phys. Plasmas* **11** 2399
[25] Angus J R, Krasheninnikov S I and Smolyakov A I 2010 *Phys. Plasmas* **17** 102115
[26] Shoucri M, Matte J P and Côté A 2003 *J. Phys. D: Appl. Phys.* **36** 2083
[27] Park G Y, You S J, Iza F and Lee J K 2007 *Phys. Rev. Lett.* **98** 085003
[28] Park G Y and Lee J K 2008 *J. Phys. D: Appl. Phys.* **41** 022004
[29] Liu Y X, Zhang Q Z, Jiang W, Hou L J, Jiang X Z, Lu W Q and Wang Y N 2011 *Phys. Rev. Lett.* **107** 055002
[30] Gu S, Kang H J, Kwon D C, Kim Y S, Chang Y M and Chuang C W 2016 *Phys. Plasmas* **23** 063506
[31] Xu L, Cheng L, Funk M, Ranjan A, Hummel M, Bravenec R, Sundararajan R, Economou D J and Donnelly V M 2008 *Appl. Phys. lett.* **93** 261502
[32] Koepke M, Ellis R F, Majeski R P and McCarrick M J 1986 *Phys. Rev. Lett.* **56** 1256
[33] Hojo H and Hatori T 1993 *J. Phys. Soc. Jpn* **62** 2212
[34] Zhang H s and Lin Z 2010 *Phys. Plasmas* **17** 072502
[35] Elfimov A G, Galvao R M O, Sgalla R J F and Smolyakov A I 2012 *39th EPS Conference on Plasma Physics, 2–6 July 2012, Stockholm, Sweden*
[36] Fu Y Y, Zheng B C, Wen D Q, Zhang P, Fan Q H and Verboncoeur J P 2020 *Plasma Sources Sci. Technol.* **29** 09LT01
[37] Giruzzi G, Artaud J F, Dumont R J, Imbeaux F, Bibet P, Bergerby G, Bouquey F, Clary J, Darbot C, Ekedahl A, Hoang G T, Lennholm M, Maget P, Magne R, Segui J L, Bruschi A and Granucci G 2004 *Phys. Rev. Lett.* **93** 255002
[38] Yang Y L, Xiang N and Hu Y M 2017 *Phys. Plasmas* **24** 082503
[39] Zhai X M, Chen J L, Xiang N, Bonoli P T and Shiraiwa S 2019 *Phys. Plasmas* **26** 052509
[40] Anderegg F, Affolter M, Kabantsev A A, Dubin D H E, Ashourvan A and Driscoll C F 2016 *Phys. Plasmas* **23** 055706
[41] Chen L J, Maldonado A, Bortnik J, Thorne M, Li J X, Dai L and Zhan X Y 2015 *J. Geophys. Res.* **120** 6514
[42] Oneil T M 1965 *Phys. Plasmas* **8** 2255